nature communications

Article

https://doi.org/10.1038/s41467-025-64691-6

Conservative port-to-port funneling of light in nonlinear photonic lattices

Received: 30 June 2025

Accepted: 24 September 2025

Published online: 03 November 2025

Check for updates

Georgios G. Pyrialakos[1], Hediyeh M. Dinani[1], Do Hyeok Jeon[1], Majid G. Nazarlu[1], Huizhong Ren[1], Abraham M. Berman Bradley[1], Mercedeh Khajavikhan[1,2] & Demetrios N. Christodoulides[1,2]

Photonic systems that steer, guide, or focus light at the microscale are usually designed under passive and lossless conditions. However, Hermiticity, which governs wave evolution in such conservative environments, strictly limits how light can propagate and flow, preventing power from orthogonal inputs to merge into a single coherent channel. Here, we show that this fundamental barrier can be overcome through a nonlinear wave-dynamic process inaccessible under linear Hermitian conditions—the conservative funneling of light. We conceptualize this effect as an all-optical thermodynamic process, whereby wave packets, regardless of origin or coherence, are carried toward the lattice center and combine into a localized ground state. We identify a parametric regime of high powers where kinetic and nonlinear photon energies facilitate the irreversible transport of optical power. Our results demonstrate >70% port-to-port efficiency in a 20-channel system, establishing a robust framework for a universal, fully conservative light funnel.

One of the primary objectives in photonics is to develop new strategies for controlling and directing the flow of light[1]. Over the years, innovative approaches have continually emerged, leveraging increasingly sophisticated degrees of freedom while propelling fields like non-Hermitian and topological photonics to the forefront of research[2,3]. This progress has unveiled a plethora of novel wave-dynamic phenomena, from topologically-protected propagation and exceptional point dynamics, to metamaterial and plasmonic interactions[4–10]. Yet, despite this progress, one unique wave-dynamic response has remained out of reach in optics: the conservative and faithful funneling of light. Fundamentally, this prospect is barred by the laws of Hermiticity, which strictly prohibit the universal convergence of power from mutually orthogonal inputs into a single predesignated port, even in the presence of nonreciprocity. In other words, in the linear domain, it is impossible to devise a transmission or scattering matrix that can both result in optical funneling and remain unitary. This restriction underpins the operation of all linear lossless and passive systems, from integrated on-chip photonic couplers and multiplexers to waveguide arrays and cavity networks. At this point, a question naturally arises as to whether a truly conservative funnel for light is possible. If successful, this prospect could unlock a unique potential for directed energy and light guiding applications, offering alternative methods for controlling light concentration and precision, attributes crucial for the fields of imaging, communications, and sensing.

To tackle this challenge, nonlinearity emerges as the only available pathway. However, taming the response of nonlinear optical configurations supporting multiple orthogonal degrees of freedom becomes extremely challenging, as information about their long-term behavior can only be inferred statistically or thermodynamically[11,12]. Recently, a self-consistent optical thermodynamic theory has been proposed to address these challenges and provide deeper insights into the physics of multimode nonlinear optical systems[13–20]. Grounded in entropic principles, this framework provides precise criteria for predicting the equilibrium states of light, offering a different perspective on previously observed phenomena in nonlinear optics, such as beam self-cleaning in multimode fibers[21–24]. Within this framework, light propagation is governed by conservation laws, which, under certain conditions, can be harnessed to favorably manipulate the modal content of light. In this context, recent experimental studies have demonstrated that nonlinear light Joule-Thomson expansion in a

[1]Ming Hsieh Department of Electrical and Computer Engineering, University of Southern California, Los Angeles, CA, USA. [2]Department of Physics and Astronomy, University of Southern California, 825 Bloom Walk, Los Angeles, CA, USA. e-mail: gp_019@usc.edu; demetri@usc.edu

photonic array can faithfully steer the injected optical power into the system's fundamental mode, following a balanced exchange between the kinetic and nonlinear components of the optical Hamiltonian energy[25,26]. On the theoretical front, the principles of optical thermalization can describe multimode topological, orbital angular momentum (OAM)[27,28], and non-Hermitian systems[29,30], including the exotic regime of negative temperatures[31,32].

Building on these fundamental principles, in this work, we develop and demonstrate a conservative funnel for light, where power can be directed with high efficiency from any input into a single predesignated localized output. This effect manifests itself in judiciously crafted potential distributions that support localized lower-order modes in the central region of a nonlinear lattice. The formation of stable funnel paths relies on a balanced exchange between the kinetic and nonlinear components of the optical Hamiltonian energy, facilitating rapid cooling of light to near-zero temperatures. In optical thermodynamics, a low temperature indicates that optical power has condensed almost entirely into the lower-order modes, resulting in a thermally locked Rayleigh-Jeans state that displays minimal microcanonical fluctuations[33]. This response not only promotes the global convergence of light power to the center of the lattice but also ensures the stability of the funneled path. By carefully tailoring the effective potential profile of a lattice, we demonstrate a highly efficient, fully conservative router that consistently directs light to a single port, regardless of the input excitation conditions. The principles of conservative light funneling are universal and can, in principle, be applied in various nonlinear optical platforms, from 2D fiber arrangements to on-chip planar integrated systems.

Results

Problem formulation

Figure 1 illustrates the general laws of light transmission in a photonic array. Within a tight-binding formalism, the system is described by:

$$id_z a_n + \sum_{m\neq n} H_{nm} a_m + \Delta_n a_n + |a_n|^2 a_n = 0, \tag{1}$$

where a_n denotes the complex amplitude of the optical field at site n, and $\hat{H}$ corresponds to a tridiagonal Hamiltonian matrix with off-diagonal elements H_{nm} representing nearest neighbor couplings while the diagonal signifies a local index detuning $\Delta_n = H_{nn}$ acting as an effective local potential at site n. Finally, the last term describes the Kerr nonlinearity in this system. Each waveguide element in this array is assumed to be single-mode. Note that in this local basis, each port specifies an orthogonally independent vector. Under linear conditions, the transmission matrix that relates incoming and outgoing waves is given by $\hat{T} = e^{-i\hat{H}L}$ for an array of length L.

In the absence of gain and loss, the transmission matrix $\hat{T}$ remains unitary, ensuring that waves injected at independent input ports (I_1, I_2, I_3 in Fig. 1a) are mapped to mutually orthogonal output states (O_1, O_2, O_3 in Fig. 1a) (see *Methods* for a rigorous proof). This fundamental principle governs the dynamics of all conservative linear systems, including non-reciprocal and z-variant configurations, inherently preventing the convergence of power from orthogonal inputs into a single output port. One possible way to overcome this limitation is to employ non-Hermitian approaches (Fig. 1b). Specifically, introducing gain directly into a target channel or the coupling itself can result in an apparent funneling-like effect[34]. However, such non-Hermitian methodologies inherently favor light amplification or filtering—processes that are fundamentally distinct from an actual transmission of power. In this respect, to realize a funnel for light, one must move beyond non-Hermitian schemes and instead explore such possibilities in conservative nonlinear environments. In the presence of nonlinearity, light evolution is no longer bound by the spectral structure of the optical array, as power can freely flow between modes through wave-mixing processes. Consequently, the orthogonality of the outputs can be broken, enabling multiple independent input states to converge into a common channel while preserving a conservative, unitary response (Fig. 1c). Herein, the challenge lies in designing a system where this unique behavior is promoted through nonlinearity.

Figure 2 illustrates the core principles underlying the funneling response as conceptualized in this study. Our approach is enabled in judiciously designed photonic arrays, where a uniform detuning difference, $\Delta = \Delta_n - \Delta_{n-1}$ is continuously applied across the guiding elements, generating a triangular effective potential with a peak at the center of the array. The optimal detuning range lies below $\Delta < 0.1$, corresponding to a shallow index gradient. To understand the role of this design, we must first examine the system's eigenvalues and eigenmodes. In this lattice, the supermodes with the highest propagation constants, β_0, are localized near the potential peak, while higher-order supermodes extend progressively toward the system's outer boundaries. In discrete lattices, this eigenmode structure is typically associated with Bloch oscillations[35]. Our strategy for designing a conservative funnel for light focuses on identifying a nonlinear parametric regime that enables a unidirectional transfer of power from higher-order supermodes, localized away from the potential peak, into lower-order states at the center of the array. Crucially, this response must unfold independently of the initial input conditions and mode

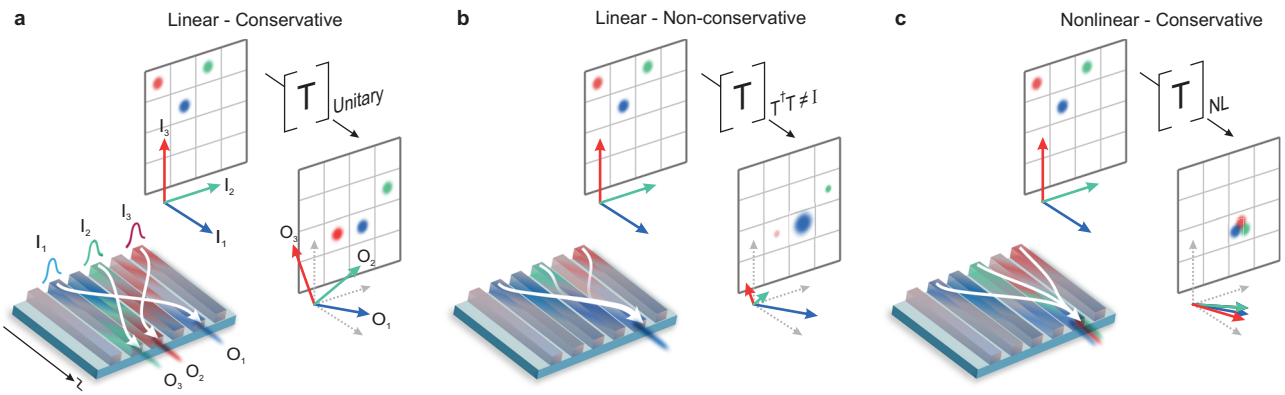

Fig. 1 | Principles of light transmission in optical arrays. a In lossless and passive configurations, the transmission matrix T performs a norm-preserving rotation of the input states, here represented by the colored arrows. In this scenario, a funneling response is prohibited, as power transfer between input I and output O states is locked between orthogonal pairs. **b** By introducing gain and/or loss, light can be selectively attenuated or amplified, resulting in an apparent flow of light towards a universal output. Here, the blue output may represent a lasing state of the array. **c** A true optical funnel requires a nonlinear transmission matrix, enabling the unrestricted flow of power from mutually orthogonal input states towards non-orthogonal states.

https://doi.org/10.1038/s41467-025-64691-6

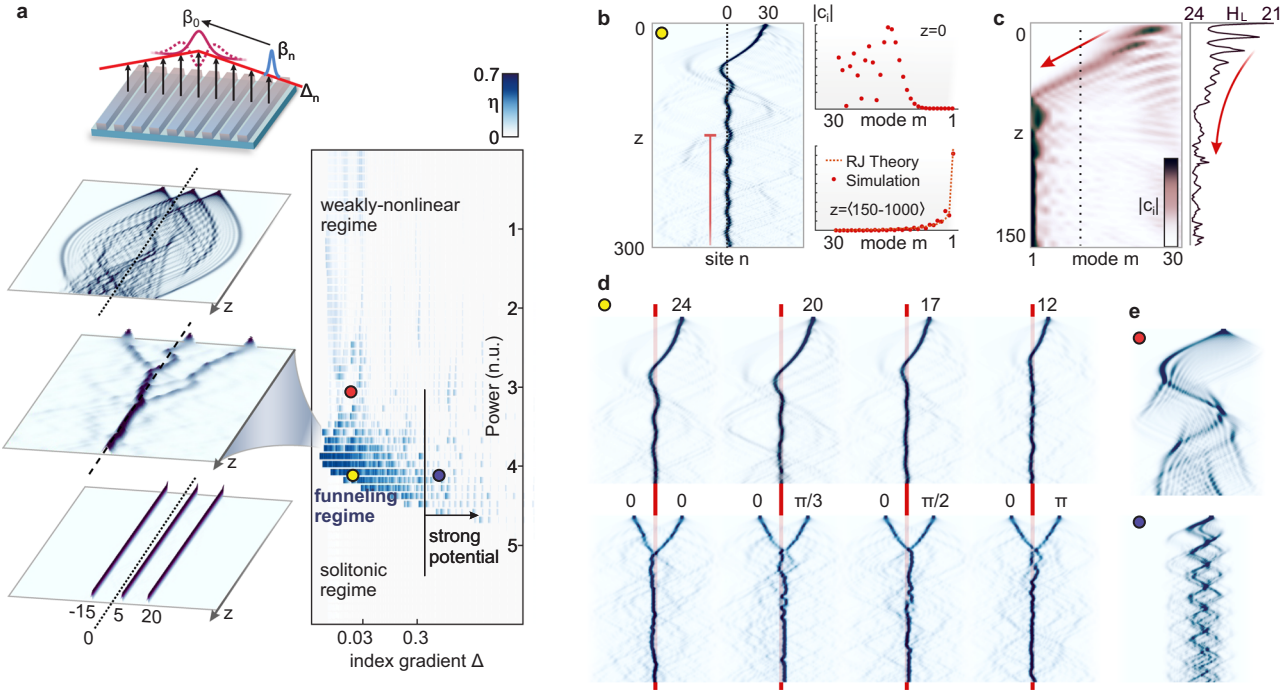

Fig. 2 | Principles of light funneling in nonlinear arrays. a An array with a weak linear index gradient Δ exhibits localized ground states at the peak of its effective potential. Within a certain range of power P, the nonlinear dynamics realize an optical funnel for light. In the scenario depicted, light is injected from 3 input ports and undergoes nonlinear evolution at three power regimes, (top) Bloch oscillations, (middle) funneling dynamics, (bottom) soliton dynamics. The η parameter serves as an efficiency metric, measuring the ratio of power accumulated at the funneling point (within the FWHM of the fundamental mode) to the total injected power. **b** Example of single-port injection at the funneling regime (Δ=0.043, P = 4.1). At the input, light occupies several higher order-modes. At the output, the field collapses irreversibly into a thermal state characterized by a Rayleigh-Jeans distribution at near zero temperatures. The modal occupancies are averaged along the red line. **c** Evolution of the modal amplitudes during funneling. Power progressively flows towards lower order modes, following a drop of the linear Hamiltonian energy H_L. **d** Light evolution for arbitrary input ports (top panels) at Δ = 0.043 and P = 4.1 (yellow dot denotes the respective parameter point in map (**a**). Numbers indicate the individual injection ports. Double-port injections (bottom panels) are shown for various input phases indicated by the number pairs. **e** Dynamics beyond the funneling regime for different injection ports. The colored dots denote the respective parameter points in map (**a**).

distribution at $z = 0$. As we will see in the subsequent section, this strategy relies on a conceptual understanding of the energetic and thermodynamic laws that govern nonlinear evolution in such multimode structures.

Principles of light funneling

To gain a deeper insight into the funneling response, we must first examine the energetic principles that govern the nonlinear dynamics of Eq. (1). The array of Fig. 2a comprises M coupled channels, thus supporting a corresponding total of M lattice supermodes. In our array, these modes typically extend across several neighboring sites but remain largely localized. In this configuration, evolution remains conservative, where both the total optical power, $P = \sum_n |a_n(z)|^2$ and the total Hamiltonian energy $H_{tot} = H_L + H_{NL}$ are preserved. The first component of the Hamiltonian energy, $H_L = \sum_i \beta_i |c_i(z)|^2$, represents the contribution from linear evolution, where β_i denotes the propagation constant of supermode i with the complex modal amplitude of $c_i(z) = \langle u_i | a \rangle$ where $|u_i\rangle$ is the eigenmode i. The magnitude of this linear energy component reflects the distribution of light among the various supermodes, with higher values indicating a more probable occupancy of supermodes with larger propagation constants, which are localized closer to the potential peak. In contrast, the second energy component $H_{NL} = 1/2 \sum_n |a_n(z)|^4$ arises from the Kerr nonlinearity and quantifies the nonlinear interaction energy. Notably, H_{NL} serves as a measure for the spatial concentration of light, due to its quartic dependence on $|a_n|$, with higher values suggesting that optical power is confined to fewer guiding elements at higher peak amplitudes. Since H_{tot} is strictly conserved along the propagation axis z, the two components of the total Hamiltonian energy must fluctuate in perfect balance, i.e., $dH_L/dz = -dH_{NL}/dz$.

By considering these key theoretical aspects, let us now investigate the conditions under which funneling dynamics can emerge in a lattice with a weak triangular potential. We begin with an illustrative example (shown in Fig. 2a), where light is simultaneously injected into three independent input ports of an array with a normalized index gradient Δ = 0.06. When light is injected into the array at low power levels, the system exhibits a quasi-linear response, characterized by weakly interacting Bloch oscillations. As the optical power at the input is increased, oscillations are suppressed, and light begins to gravitate towards the center of the array. This corresponds to the funneling regime. Beyond a certain power threshold, the funneling effect diminishes, and a stronger nonlinearity leads to the formation of solitons, which propagate along static trajectories. Clearly, for this selected value of Δ, a funneling response is successfully stimulated within a certain range of guided powers P. By conducting an extensive number of simulations, treating both Δ and P as free parameters we can distinctly pinpoint this parameter space, as presented in Fig. 2a. It is important to note that, although this map is derived under specific input conditions (with only the input power varying), it remains universal and independent of the input ports.

To contextualize this unique response within the theoretical framework discussed here, we examine a more simplified example in greater detail (Fig. 2b). Here, light is injected into the array through a single input port, while the system is optimally tuned within the previously identified funneling regime (at the yellow dot of Fig. 2a). Near the input, light remains confined within a soliton-like structure with a

high peak amplitude, characterized by a high nonlinear energy component H_{NL}. Positioned 30 sites away from the potential peak, the wave envelope occupies several higher-order modes. As propagation ensues along z, light starts to disperse linearly across the lattice, a process accompanied by power radiation due to nonlinear Peierls-Nabarro effects[36,37]. This interplay between linear and nonlinear effects leads to a gradual reduction of the peak amplitude, causing a decrease in H_{NL} and a proportional increase of H_L, like what is observed during an optical JT expansion. This nonlinear process facilitates a shift of power towards lower-order modes, which are weighted towards the left, forcing light closer to the potential peak. In other words, the funneling regime establishes favorable dynamic conditions for a nearly optimal transfer of power from higher-order modes, localized near the injection port, toward the fundamental mode of the lattice. The origin of this effect and its interpretation as a JT thermodynamic expansion process are discussed comprehensively in Supplementary Note 1.

When light reaches the center of the array, it attains thermal equilibrium, ensuring the irreversible confinement of power along the funneled path. In other words, irreversibility is established by the collapse of the wave-field into a thermal-entropic state, characterized by a very low optical temperature, as defined within the framework of optical thermodynamics. In this state, the modal occupancies relax into a Rayleigh-Jeans (RJ) distribution

$$\left\langle |c_i|^2 \right\rangle = \frac{T}{\beta_i + \mu} \tag{2}$$

where T corresponds to the optical temperature and μ to the optical chemical potential. In the context of optical thermodynamics, a zero temperature indicates that optical power has condensed fully into the ground state, whereby nonlinear mode-mixing processes substantially diminish in strength. To verify the emergence of this thermal RJ state, we calculate the theoretically expected values of T and μ from the associated set of extensive variables (H_L, P) of the collapsed wave packet, for the case presented in Fig. 2b (see Supplementary Note 2 for the methodology). By substituting T and μ into Eq. 2, we acquire the RJ distribution, plotted as the dashed curve in Fig. 2b. This theoretical curve matches the simulated modal occupancies (red dots), which correspond to the averaged power per mode along the funneled path from $z = 150$ to $z = 1000$. This result confirms the thermalization process, which underpins the irreversible nature of the funneling response.

The universality of light funneling is exemplified in Fig. 2c with various excitation scenarios shown at the same values of Δ and P. Remarkably, at optimal input power, light consistently converges toward the center of the array regardless of the excitation port, as illustrated in the top row, highlighting the fundamental essence of an optical funnel. The second row presents results for dual-port excitations, affirming the nonlinear nature of the phenomenon, which overrides linear interference effects. In other words, the system can reliably funnel light to the center, irrespective of the relative phase between inputs in multi-port excitation scenarios. However, it is important to note that the theoretical framework presented here is based on the energetic response of isolated wavepackets and does not incorporate nonlinear interactions between independently launched excitations. This limitation becomes relevant when closely spaced input ports are simultaneously excited: in such cases, the funneling behavior may break down, requiring a different power regime to restore it. These aspects are further explored in Supplementary Note 3 and Supplementary Note 4, while funneling in bilayer lattices is examined in Supplementary Note 5.

Figure 2d shows two examples where the two parameters (P, Δ) fall just outside their optimal range. At low input powers, the Hamiltonian energy is insufficient for trapping light at the potential peak; consequently, the Bloch oscillations persist, and the wave packet eventually disperses. Moreover, if the slope of the potential is too steep, the nonlinear energy decays too rapidly, and light becomes trapped again in Bloch oscillations before reaching the center, disrupting its trajectory. In both scenarios, light fails to lock thermally and energetically at the potential peak.

Port-to-port funneling of light

The phenomenon of light funneling demonstrated in this work constitutes more than a unique wave-dynamic effect. It establishes fundamental principles for steering and focusing light at the microscale, where geometric optics no longer apply and coherence effects dominate. These insights can be leveraged to design a universal high-power router for light, capable of directing optical power from any input into a common predetermined output port. The examples presented in Fig. 2 clearly illustrate that an array operating within the funneling regime can faithfully channel optical power toward its center, where light is ultimately captured by the system's lower-order modes. However, within the funneling regime, the fundamental supermode assumes a Gaussian-like profile with an FWHM occupying, on average, six guiding sites at the peak of the potential. Consequently, port-to-port transmission efficiency remains relatively low. To realize a true port-to-port router, a properly engineered design must be developed featuring a highly localized fundamental mode state, while still leveraging the core principles of light funneling outlined in the previous sections.

Figure 3 illustrates a proposed optimized design that facilitates light funneling exclusively toward the central port of the photonic array, labeled as port 0. In this array, light undergoes a two-stage evolution process. At the input, light propagates through an optical funnel, experiencing an effective potential that promotes the nonlinear response we explored in the previous section, (using the same parameter set in Fig. 2). After approximately 50 coupling lengths, the middle guiding element exhibits a raised index profile, which results in the gradual squeezing of the fundamental mode into a tightly localized state. Under the action of nonlinearity, in a non-adiabatic manner, the power already trapped in the funnel rapidly condenses into this middle site, always exiting from the middle port. In the eight examples presented in Fig. 3, efficiency ranges between 68% (for the furthest input) and 81%. The optimized design shown in Fig. 3 can also be leveraged to improve the stability and efficiency of the dual-injection scenario, as demonstrated in Supplementary Note 6, where the first two dual-input cases from Fig. 2c are replicated. In these cases, which involve twice the power of the single-input scenarios, self-focusing can occasionally compete with RJ thermalization at the funnel point, resulting in the deviations observed in Fig. 2c.

Discussion

Having completed our conceptual design, we continue to assess the practical applicability of our model. The funneling regime lies just below the soliton collapse threshold, a characteristic that may guide us toward potential platforms for designing light funnels. In other words, a light funnel can form in photonic arrays that support variable index distributions and can sustain power levels close to the solitonic regime. Here, solitons refer to discrete lattice solitons rather than temporal or spatial solitons. The latter typically emerge at much higher power levels dictated by the material's self-focusing collapse threshold.

In Fig. 4, we numerically investigate funneling dynamics in a fused silica platform[38] of a weakly-guiding photonic waveguide array, treated as a full-wave problem in the paraxial regime. This platform enables precise inscription of waveguide elements with arbitrary weak variations in their index potential, across both the transverse plane and the propagation direction z[8]. Using experimentally accessible parameters, we can replicate the funneling response by injecting light into different ports at 250 kW—a power level recently used to observe the Joule-

https://doi.org/10.1038/s41467-025-64691-6

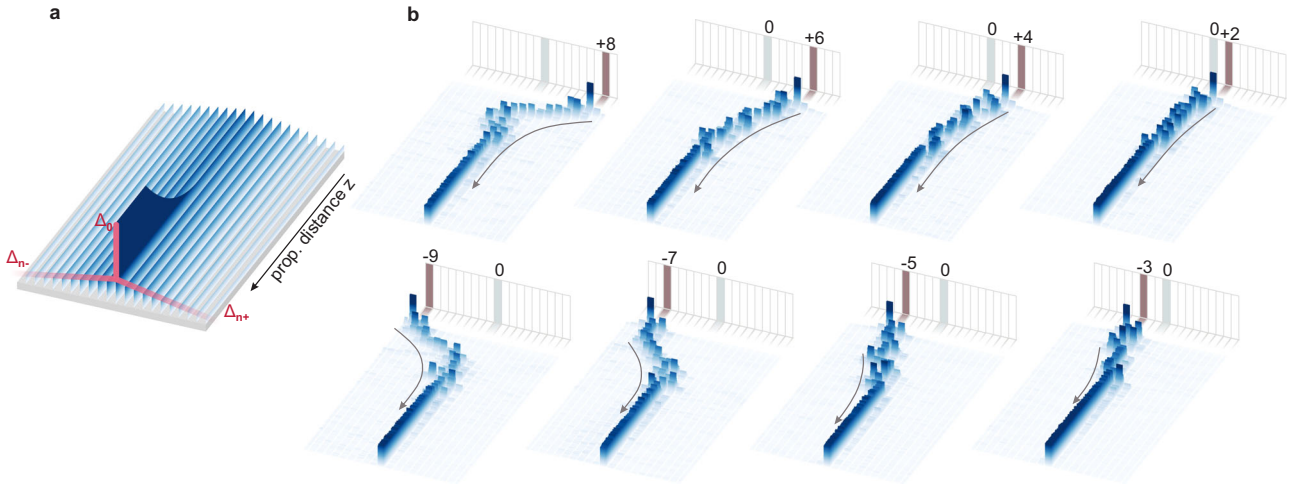

Fig. 3 | A universal port-to-port router for light. a An optical array with a detuning parameter $\Delta = 0.043$, designed to support funneling dynamics at appropriate power levels. After approximately 50 coupling lengths, the central waveguide exhibits an increased refractive index, collapsing the ground state into a single site. **b** Port-to-port funneling is demonstrated using the array shown in (**a**) establishing a universal light router that irreversibly captures power from any input port. Port indices are labeled relative to the designated funneling port (0): positive to the right and negative to the left.

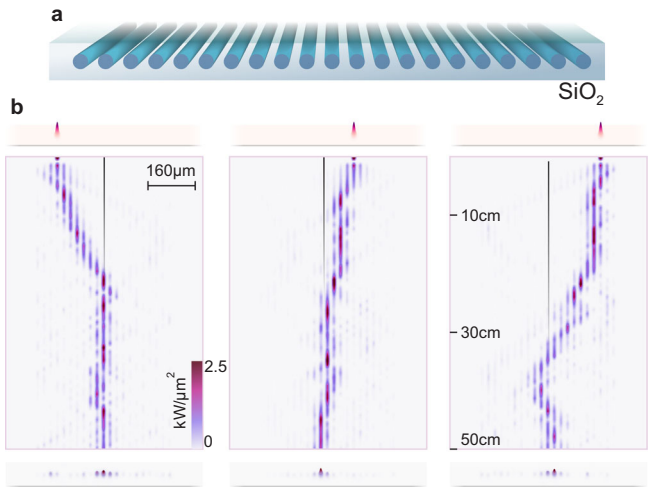

Fig. 4 | Proposed experimental setup. a A 1D array of evanescently coupled waveguides on a fused silica sample, designed with the following parameters: waveguide radius $a = 7\mu m$, core-to-core distance $r = 19.6\mu m$, refractive index difference $\Delta n = n_{core} - n_{clad} = 0.5 \times 10^{-3}$, $n_{clad} = 1,457$, wavelength $\lambda = 800nm$. The waveguides follow a 5th-order super-Gaussian profile and the index gradient between neighboring elements is set at $1\%\Delta n$. **b** Beam propagation method simulations of light funneling at $P \approx 250kW$.

Thomson thermodynamic expansion of light on the same platform. The waveguides are excited by Gaussian inputs that exhibit non-zero spatial overlaps and are thus not strictly orthogonal, in contrast to the local basis vectors of Eq. (1). In more advanced platforms, the effective potential, in principle, can be controlled via electro-optic or thermo-optic effects, as demonstrated in experiments conducted on integrated and on-chip photonic configurations[39,40].

In conclusion, the optical funnel introduces a unique capability in nonlinear optics, enabling power-directed transport beyond the orthogonality constraints of linear systems. Unlike photonic lanterns[41,42], which perform adiabatic mode transformations while matching the number of input and output channels (either in local or supermode basis), the optical funnel leverages nonlinear dynamics to steer power into the same self-orthogonal state from multiple independent channels. It also surpasses the limitations of linear couplers, which typically require active switching and prior knowledge of the input channel or state, even in the simplest 2-to-1 configurations.

In this context, we envision that high-power funnels could be incorporated in nonlinear environments based on state-of-the-art highly nonlinear materials, such as AlGaAs or Si, paving the way for efficient on-chip integration. Owing to their significantly stronger nonlinear response, these platforms could reduce the required power levels by several orders of magnitude compared to conventional silica-based systems, where stimulated Raman scattering can pose practical concerns. More broadly, the power threshold for entering the funneling regime is fundamentally governed by the interplay between the linear and nonlinear components of the system's Hamiltonian, and is therefore directly linked to the coupling strength. Designing a slower array, i.e., one with reduced inter-site coupling, can further suppress the power requirement, albeit at the cost of longer propagation distances, highlighting an inherent trade-off.

Beyond optics, the principles of funneling can be potentially observed in other nonlinear settings, such as Bose-Einstein condensates, superconducting platforms, and magnonic systems[43–46]. On the theoretical front, our work demonstrates that the thermodynamic principles derived from a Hamiltonian formulation of nonlinear optics open up a vast, largely unexplored landscape, where unique dynamical effects may emerge and be harnessed for practical applications in optics and beyond.

Methods

Transmission properties of Hermitian, non-Hermitian, and nonlinear environments

All passive and lossless linear wave-dynamic systems, from waveguiding configurations to scattering environments or networks, are inherently characterized by a unitary transmission or scattering operator U (generalizing the transmission matrix T of the main manuscript). This matrix satisfies the condition

$$U^{\dagger}U = I, \tag{3}$$

where $U^{\dagger}$ is the conjugate transpose of U, and I is the identity matrix. This means that unitary matrices preserve inner products and thus maintain the norm of vectors, a property that underpins the dynamics of Hermitian systems, as conceptualized in Fig. 1a. To prove this statement, it is adequate to show that for two orthogonal inputs $|I_2\rangle$,

$|I_1\rangle$ (i.e., $\langle I_1, | , I_2\rangle = 0$) the outputs $|O_2\rangle$, $|O_1\rangle$ will also be orthogonal. Using Eq. M1,

$$\langle O_1|O_2\rangle = \langle U I_1|U I_2\rangle = \langle I_1|U^\dagger U|I_2\rangle = \langle I_1|I_2\rangle = 0 \quad (4)$$

which clearly validates the previous argument. This suggests that when a system is engineered to fully couple a specific input and output port, any power injected at other input ports cannot reach that output. In other words, the power injected at non-designated ports will be fully isolated from the intended output, even if time-reversal symmetry and reciprocity are violated. The same principles apply to systems with a spatially varying (or time-dependent) evolution operator or Hamiltonian $\hat{H}(z)$, in which case the transmission or scattering operator takes the form $U(L,0) = \mathscr{T}\exp\left(-i\int_0^L \hat{H}(z)dz\right)$, where $\mathscr{T}$ is the time-ordering operator (or more precisely, path-ordering along the propagation axis z). This generalized operator governs the dynamics in non-uniform or modulated structures, and remains unitary and independent of the specific input, as expected for a linear system, thus obeying both Eq. 3 and Eq. 4

In contrast, non-Hermitian environments do not satisfy Eq. 3, implying that a system can allow multiple inputs to share a common output channel. For example, this effect becomes feasible near high-order Exceptional Points, where the spectrum collapses around the vicinity of a single eigenvector—which, in principle, can be tailored to correspond to a predesignated output port. As argued in the main manuscript, in all such environments, the underlying mechanism that can promote an apparent funneling response is the action of gain and loss. This extends to all pseudo-Hermitian systems (such as the Hatano-Nelson lattice) where unidirectional amplification induces a funneling-like behavior. In these systems, power is selectively attenuated in one direction and amplified in the other as light propagates through the array[34].

As a consequence of the previous arguments, to realize a true optical funnel, one must employ a nonlinear transmission matrix that is inherently free from gain and loss. In such systems, the nonlinear transmission matrix remains unitary (i.e., it satisfies Eq. 3), but Eq. 4 no longer applies because the unitary operator U becomes input-dependent due to the system's nonlinear nature. Thus, in principle, a truly conservative and unitary funneling response is no longer prohibited.

Data availability

The data that support the findings of this study are available from G.G.P.

Code availability

The MATLAB code used to implement the port-to-port funnel presented in Fig. 3 is publicly available at: https://doi.org/10.5281/zenodo.17089999. Additional codes supporting other results are available from G.G.P. upon request.

References

1. Chen, Z. & Segev, M. Highlighting photonics: looking into the next decade. *eLight* **1**, 2 (2021).
2. Lu, L., Joannopoulos, J. D. & Soljačić, M. Topological photonics. *Nat. Photonics* **8**, 821–829 (2014).
3. Nasari, H., Pyrialakos, G. G., Christodoulides, D. N. & Khajavikhan, M. Non-Hermitian topological photonics. *Opt. Mater. Express* **13**, 870–885 (2023).
4. Vakil, A. & Engheta, N. Transformation optics using graphene. *Science* **332**, 1291–1294 (2011).
5. Plotnik, Y. et al. Experimental observation of optical bound states in the continuum. *Phys. Rev. Lett.* **107**, 183901 (2011).
6. Kildishev, A. V., Boltasseva, A. & Shalaev, V. M. Planar photonics with metasurfaces. *Science* **339**, 1232009 (2013).
7. Yu, Z. & Fan, S. Complete optical isolation created by indirect interband photonic transitions. *Nat. Photonics* **3**, 91–94 (2009).
8. Pyrialakos, G. G. et al. Bimorphic floquet topological insulators. *Nat. Mater.* **21**, 634–639 (2022).
9. Alù, A. & Engheta, N. Achieving transparency with plasmonic and metamaterial coatings. *Phys. Rev. E—Statistical Nonlinear Soft Matter Phys.* **72**, 016623 (2005).
10. Patsyk, A., Sivan, U., Segev, M. & Bandres, M. A. Observation of branched flow of light. *Nature* **583**, 60–65 (2020).
11. Zakharov, V. E., L'vov, V. S. & Falkovich, G. Kolmogorov spectra of turbulence I: wave turbulence. *Springer Sci. Bus. Media* (Springer, 2012).
12. Klaers, J., Schmitt, J., Vewinger, F. & Weitz, M. Bose–Einstein condensation of photons in an optical microcavity. *Nature* **468**, 545–548 (2010).
13. Wu, F. O., Hassan, A. U. & Christodoulides, D. N. Thermodynamic theory of highly multimoded nonlinear optical systems. *Nat. Photonics* **13**, 776–782 (2019).
14. Pourbeyram, H. et al. Direct observations of thermalization to a Rayleigh–Jeans distribution in multimode optical fibres. *Nat. Phys.* **18**, 685–690 (2022).
15. Picozzi, A. Towards a nonequilibrium thermodynamic description of incoherent nonlinear optics. *Opt. Express* **15**, 9063–9083 (2007).
16. Ramos, A., Fernández-Alcázar, L., Kottos, T. & Shapiro, B. Optical phase transitions in photonic networks: a spin-system formulation. *Phys. Rev. X* **10**, 031024 (2020).
17. Ren, H. et al. Nature of optical thermodynamic pressure exerted in highly multimoded nonlinear systems. *Phys. Rev. Lett.* **131**, 193802 (2023).
18. Baudin, K. et al. Classical Rayleigh-Jeans condensation of light waves: observation and thermodynamic characterization. *Phys. Rev. Lett.* **125**, 244101 (2020).
19. Ren, H. et al. Photon–photon chemical thermodynamics of frequency conversion processes in highly multimode systems. *Light Sci. Appl.* **14**, 188 (2025).
20. Shi, C., Kottos, T. & Shapiro, B. Controlling optical beam thermalization via band-gap engineering. *Phys. Rev. Res.* **3**, 033219 (2021).
21. Ferraro, M., Mangini, F., Zitelli, M. & Wabnitz, S. On spatial beam self-cleaning from the perspective of optical wave thermalization in multimode graded-index fibers. *Adv. Phys. X* **8**, 2228018 (2023).
22. Mangini, F., Ferraro, M., Tonello, A., Couderc, V. & Wabnitz, S. High-temperature wave thermalization spoils beam self-cleaning in nonlinear multimode GRIN fibers. *Opt. Lett.* **48**, 4741 (2023).
23. Mangini, F. et al. Statistical mechanics of beam self-cleaning in GRIN multimode optical fibers. *Opt. Express* **30**, 10850 (2022).
24. Mangini, F., Ferraro, M., Tonello, A., Couderc, V. & Wabnitz, S. Wave thermalization sets high-power limitation to spatial beam self-cleaning in multimode optical fibers. in *Laser Resonators, Microresonators, and Beam Control XXVI* (eds. Armani, A. M., Ilchenko, V. S. & Sheldakova, J. V.) 35 (SPIE, 2024) https://doi.org/10.1117/12.3007907.
25. Kirsch, M. S. et al. Observation of Joule–Thomson photon-gas expansion. *Nat. Phys.* **21**, 214–220 (2025).
26. Pyrialakos, G. G., Khajavikhan, M. & Christodoulides, D. N. Fundamental mode excitation via Joule–Thomson light expansion in nonlinear optical lattices. *Opt. Lett.* **50**, 1349–1352 (2025).
27. Wu, F. O. et al. Thermalization of light's orbital angular momentum in nonlinear multimode waveguide systems. *Phys. Rev. Lett.* **128**, 123901 (2022).
28. Podivilov, E. V. et al. Thermalization of orbital angular momentum beams in multimode optical fibers. *Phys. Rev. Lett.* **128**, 243901 (2022).
29. Pyrialakos, G. G., Ren, H., Jung, P. S., Khajavikhan, M. & Christodoulides, D. N. Thermalization dynamics of nonlinear non-Hermitian optical lattices. *Phys. Rev. Lett.* **128**, 213901 (2022).

30. Jung, P. S. et al. Thermal control of the topological edge flow in nonlinear photonic lattices. *Nat. Commun.* **13**, 4393 (2022).
31. Marques Muniz, A. L. et al. Observation of photon-photon thermodynamic processes under negative optical temperature conditions. *Science* **379**, 1019–1023 (2023).
32. Baudin, K. et al. Observation of light thermalization to negative-temperature Rayleigh-Jeans equilibrium states in multimode optical fibers. *Phys. Rev. Lett.* **130**, 063801 (2023).
33. Jeon, D. H. et al. Fluctuation statistics of nonlinear optical microcanonical systems. *Phys. Rev. Lett.* **134**, 223805 (2025).
34. Sebastian, W. et al. Topological funneling of light. *Science* **368**, 311–314 (2020).
35. Morandotti, R., Peschel, U., Aitchison, J. S., Eisenberg, H. S. & Silberberg, Y. Experimental observation of linear and nonlinear optical bloch oscillations. *Phys. Rev. Lett.* **83**, 4756–4759 (1999).
36. Morandotti, R., Peschel, U., Aitchison, J. S., Eisenberg, H. S. & Silberberg, Y. Dynamics of discrete solitons in optical waveguide arrays. *Phys. Rev. Lett.* **83**, 2726–2729 (1999).
37. Dmitriev, S. V., Kevrekidis, P. G., Sukhorukov, A. A., Yoshikawa, N. & Takeno, S. Discrete nonlinear Schrödinger equations free of the Peierls–Nabarro potential. *Phys. Lett. A* **356**, 324–332 (2006).
38. Szameit, A. & Nolte, S. Discrete optics in femtosecond-laser-written photonic structures. *J. Phys. B. Mol. Opt. Phys.* **43**, 163001 (2010).
39. Iwanow, R. et al. Arrays of weakly coupled, periodically poled lithium niobate waveguides: beam propagation and discrete spatial quadratic solitons. *Optoelect. Rev.* **13**, 113–121 (2005).
40. Iwanow, et al. Observation of discrete quadratic solitons. *Phys. Rev. Lett.* **93**, 113902 (2004).
41. Noordegraaf, D., Skovgaard, P. M., Nielsen, M. D. & Bland-Hawthorn, J. Efficient multi-mode to single-mode coupling in a photonic lantern. *Opt. Express* **17**, 1988–1994 (2009).
42. Leon-Saval, S. G., Argyros, A. & Bland-Hawthorn, J. Photonic lanterns: a study of light propagation in multimode to single-mode converters. *Opt. Express* **18**, 8430–8439 (2010).
43. Trotzky, S. et al. Probing the relaxation towards equilibrium in an isolated strongly correlated one-dimensional Bose gas. *Nat. Phys.* **8**, 325–330 (2012).
44. Anglin, J. R. & Ketterle, W. Bose–Einstein condensation of atomic gases. *Nature* **416**, 211–218 (2002).
45. Mirhosseini, M., Sipahigil, A., Kalaee, M. & Painter, O. Superconducting qubit to optical photon transduction. *Nature* **588**, 599–603 (2020).
46. Rückriegel, A. & Kopietz, P. Rayleigh-Jeans condensation of pumped magnons in thin-film ferromagnets. *Phys. Rev. Lett.* **115**, 157203 (2015).

Acknowledgements

This work was supported by the Army Research Office award on Optical thermodynamics of nonlinear multimode systems (W911NF-23-1-0312),ONR MURI award on the classical entanglement of light(Award No. N00014-20-1-2789), the Air Force Office of Scientific Research (AFOSR) Multidisciplinary University Research Initiative (MURI) award on novel light-matter interactions in topologically nontrivial Weyl semimetal structures and systems (Award No. FA9550-20-1-0322),AFOSR MURI award on programmable systems with non-Hermitian quantum dynamics (Award No. FA9550-21-1-0202), the Department of Energy (DE-SC0022282 and DE-SC0025224), W. M. Keck Foundation, MPS Simons collaboration (Simons Grant No. 733682), U.S. Air Force Research Laboratory (FA86511820019), Israel Ministry of Defense (IMOD: 4441279927), AFRL— Applied Research Solutions (S03015) (FA8650-19-C- 1692), and fellowships from the University of Southern California.

Author contributions

G.G.P. initiated the idea, developed the theory and prepared the draft. G.G.P. and H.M.D. carried out the numerical simulations. D.H.J., M.G.N., H.R., and A.M.B.B. contributed to the discussion of the results and provided feedback on the final version of the paper, under the supervision of M.K. and D.N.C.

Competing interests

The authors declare no competing interests.

Additional information

Supplementary information The online version contains supplementary material available at https://doi.org/10.1038/s41467-025-64691-6.

Correspondence and requests for materials should be addressed to Georgios G. Pyrialakos or Demetrios N. Christodoulides.

Peer review information *Nature Communications* thanks Eran Lustig, Jae Woong Yoon and the other, anonymous, reviewer(s) for their contribution to the peer review of this work. A peer review file is available.